

PAPER • OPEN ACCESS

Phase diagram of the half-filled Anderson-Hubbard model at finite temperature

To cite this article: Nguyen Thi Hai Yen and Hoang Anh Tuan 2023 *J. Phys.: Conf. Ser.* **2485** 012004

View the [article online](#) for updates and enhancements.

You may also like

- [State-of-the-art techniques for calculating spectral functions in models for correlated materials](#)

K. Hallberg, D. J. García, Pablo S. Cornaglia et al.


- [Breakdown of coherence in Kondo alloys: crucial role of concentration versus band filling](#)

Sébastien Burdin and Claudine Lacroix

- [An advanced multi-orbital impurity solver for dynamical mean field theory based on the equation of motion approach](#)

Qingguo Feng and P M Oppeneer




 The Electrochemical Society
Advancing solid state & electrochemical science & technology

243rd Meeting with SOFC-XVIII

Boston, MA • May 28 – June 2, 2023

Accelerate scientific discovery!

[Learn More & Register](#)



Phase diagram of the half-filled Anderson-Hubbard model at finite temperature

Nguyen Thi Hai Yen^{1,2}, Hoang Anh Tuan^{1,2}

¹ Institute of Physics, Vietnam Academy of Science and Technology, Vietnam

² Graduate University of Science, Vietnam Academy of Science and Technology, Vietnam

E-mail: nhyen@iop.vast.vn

Abstract. We study metal-insulator phase diagram in the half-filled disordered Hubbard model at finite temperature. We calculate the averaged local density of states at the Fermi level and the site occupation as a function of the on-site energy at finite temperature by using typical medium theory with an impurity solver of equation of motion method. Although the metallicity in the correlated metallic region changes with temperature change, the phase diagram is almost temperature independent. We find fairly good agreement between our site occupation and those obtained by the typical medium method with other impurity solver.

1. Introduction

Metal-insulator transitions (MITs) is a crucial problem in condensed matter physics. While Mott insulating state is induced by correlation, Anderson insulating phase is induced by disorder [1, 2, 3]. The investigation of the interplay between correlation and disorder is a challenge for physicists. For the Mott MIT, the arithmetic averaged value of local density of states (LDOS) at the Fermi level is enough to describe the transition, but it can not be used as an order parameter for Anderson localization [4, 5]. In the disordered system, the most probable value or "typical value" of the LDOS instead of the arithmetic averaged one is suited to detect the Anderson MIT. Then Dobrosavljevic and co-workers have proposed the typical medium theory (TMT), where the typical density of states approximately equal to the geometric mean of LDOS [6]. The dynamical mean field theory (DMFT) with TMT method have been successfully applied to study the metal-insulator phase diagram in disordered and correlated systems [7, 8, 9, 10, 11, 12, 13].

Most of studies on MIT in the Anderson-Hubbard model (AHM) has been performed at zero temperature. In 2015, H. Braganca and co-workers [14] investigated the phase diagram of the half-filled AHM at finite temperature, focusing on the coexistence region associated with the Mott phase transition. To solve this problem they have used TMT-DMFT with the iterative perturbation theory (IPT) as an impurity solver. In our previous works, we have shown that the equation of motion method (EOM) is the fast and reliable impurity solver for TMT-DMFT at zero temperature [11, 12, 13]. In this paper we apply this method to study the metal-insulator phase diagram in the half-filled disordered Hubbard model at finite temperature.

The paper is structured as follows. In Section 2 we briefly present the TMT-DMFT for AHM model, where we use the equations of motion method as an impurity solver. In Section 3 the



averaged LDOS at the Fermi level, the site occupancy as well as the phase diagram at finite temperature are calculated and discussed. The final Section 4 contains the conclusions.

2. Model and Method

The Anderson-Hubbard model with site energies is defined by the following Hamiltonian

$$H = -t \sum_{\langle ij \rangle \sigma} (c_{i\sigma}^\dagger c_{j\sigma} + c_{j\sigma}^\dagger c_{i\sigma}) + \sum_{i\sigma} (\varepsilon_i - \mu) n_{i\sigma} + U \sum_i n_{i\uparrow} n_{i\downarrow}, \quad (1)$$

where $c_{i\sigma}^\dagger$ ($c_{i\sigma}$) is the creation (annihilation) operator of an electron at site i with spin σ . $n_{i\sigma}$ is the number particle operator, μ is the chemical potential, and t is the hopping amplitude between nearest neighbor sites i and j . U is the on-site Coulomb interaction and the local impurities ε_i are randomly variables. We assume a box distribution for energy impurities ε_i as follows $P(\varepsilon_i) = \theta(\delta/2 - |\varepsilon_i|)/\Delta$, where θ is the step function. Δ measures the strength of structural disorder.

In the DMFT, the lattice model is mapped onto a single impurity (with a random energy) embedded into the bath of non-interacting electrons, which needs to be calculated self-consistently. The coupling between the single impurity and the DMFT bath is described by the hybridization function $\eta_\sigma(\omega)$. We restrict our study to the paramagnetic case at half-filling, for which $\mu = U/2$, the hybridization function and the impurity Green function are spin independent so the spin indexes are omitted. The impurity Green function can be approximately obtained from decoupling the equations of motion as follows [15]

$$G(\omega, \varepsilon_i) = \frac{1 - \langle n_i \rangle / 2}{\omega - \varepsilon_i + U/2 - \eta(\omega) + U\eta_1(\omega)[\omega - \varepsilon_i - U/2 - \eta(\omega) - \eta_3(\omega)]^{-1}} + \frac{\langle n_i \rangle / 2}{\omega - \varepsilon_i - U/2 - \eta(\omega) - U\eta_2(\omega)[\omega - \varepsilon_i + U/2 - \eta(\omega) - \eta_3(\omega)]^{-1}}. \quad (2)$$

The "self-energies" $\eta_1(\omega)$, $\eta_2(\omega)$, $\eta_3(\omega)$ are temperature dependent [15], they describe a resonant coupling of site i with the DMFT bath and can be expressed through the hybridization function as below

$$\eta_l(\omega) = \int_{-\infty}^{+\infty} \eta(\omega) F_l(z) \left(\frac{1}{\omega - z} + \frac{1}{\omega - 2\varepsilon_i + z} \right) dz, \quad (3)$$

where $l = 1, 2, 3$. $F_1(z) = f(z) = \frac{1}{1 + \exp(z/T)}$ is the Fermi function, $F_2(z) = 1 - F_1(z)$, and $F_3(z) = 1$. The site occupation at finite temperature

$$\langle n_i \rangle = -\frac{2}{\pi} \int_{-\infty}^{\infty} f(\omega) \text{Im}G(\omega, \varepsilon_i) d\omega. \quad (4)$$

The local density of states is given by

$$\rho(\omega, \varepsilon_i) = -\frac{1}{\pi} \text{Im}G(\omega, \varepsilon_i), \quad (5)$$

The typical density of states (TDOS) can be calculated via the geometrically averaged LDOS

$$\rho_{typ}(\omega) = \exp \left[\int d\varepsilon P(\varepsilon) \ln \rho(\omega, \varepsilon) \right]. \quad (6)$$

The arithmetically averaged local density of states (ADOS) is given as

$$\rho_{arith}(\omega) = \int d\varepsilon P(\varepsilon)\rho(\omega, \varepsilon). \quad (7)$$

The typical Green function is computed by the Hilbert transform

$$G_{typ}(\omega) = \int d\omega' \frac{\rho_{typ}(\omega')}{\omega - \omega'}. \quad (8)$$

The lattice Green function can be calculated from the self-energy $\Sigma(\omega)$ and the non-interacting density of states $\rho_0(\omega)$:

$$G(\omega) = \int d\omega' \frac{\rho_0(\omega')}{\omega - \Sigma(\omega) - \omega'}, \quad (9)$$

where the self-energy $\Sigma(\omega)$ of effective medium is determined from the Dyson equation

$$\Sigma(\omega) = \omega + \mu - \eta(\omega) - G(\omega)^{-1}. \quad (10)$$

The self-consistent DMFT loop is closed by demanding the lattice Green function must be equal to the typical Green function

$$G(\omega) = G_{typ}(\omega). \quad (11)$$

We assume that our system is defined in a Bethe lattice with infinite connectivity, the non-interaction density of states $\rho_0(\varepsilon) = 4\sqrt{1 - 4(\varepsilon/W)^2}/(\pi W)$ with bandwidth W , for which the hybridization function is given by

$$\eta(\omega) = \frac{W^2}{16} G(\omega). \quad (12)$$

3. Results and Discussion

We numerically solve the equations (2)- (12). In this work, we choose the bandwidth W as the unit of energy and the Fermi level as the origin of energy axis. For the set of parameters T, U , and Δ , the possible phases of the system can be classified as follows: 1) nonzero value of $\rho_{typ}(0) \neq 0$ and $\rho_{arith}(0) \neq 0$ denote a metallic phase; 2) $\rho_{typ}(\omega) = 0$ for all ω indicates an Anderson insulating phase (gapless); and 3) a Mott insulating phase (hard gap) is signaled by $\rho_{typ}(0) = 0, \int \rho_{typ}(\omega)d\omega \neq 0$. Firstly, we consider the influence of temperature on ADOS and TDOS at the Fermi level, which characterize the metallicity of the system. In Fig.1 we plot ADOT and TDOS at the Fermi level as a function of disorder strength Δ at two values of T and for $U = 0.5$. It can be seen that, both of these values decrease as Δ increases and the effect of temperature is relatively small. For $\Delta \approx 2.5$, the ADOS at the band center is finite, while the TDOS one approaches to zero, so this may be an evidence of MIT. For larger interaction $U = 1.5$ case, as shown in Fig. 2, both of ADOS and TDOS at the Fermi level are finite for $1.0 < \Delta < 2.5$, it indicates that with increasing disorder two transitions from an insulator via a metal to an Anderson insulator are found. The ADOS and TDOS at the Fermi level slightly decrease as temperature is increased due to thermal fluctuation.

Both of ADOS and TDOS at the Fermi level as a function of interaction U at two values of T is shown in Fig. 3 for $\Delta = 1.0$ and in Fig. 4 for $\Delta = 2.0$. In each figure, the two curves have almost the same behavior and a significantly difference between them is found only for intermediate interactions with the larger values at zero temperature. Therefore, the critical interactions at which $\rho_{typ}(0)$ or/and $\rho_{arith}(0)$ vanish, are almost independent on temperature. In Fig.5 we present the phase diagram for the half-filled AHM at $T = 0.2$. Similar to the case $T = 0$, this

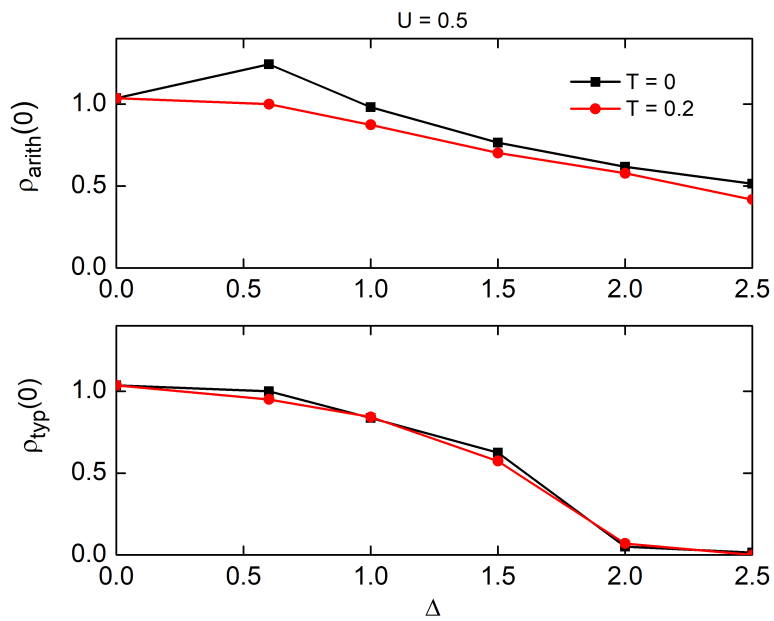


Figure 1. Arithmetic-averaged and typical DOS at the Fermi level as a function of disordered strength for $U = 0.5$ at $T = 0, 0.2$. Energy scale: $W = 1$.

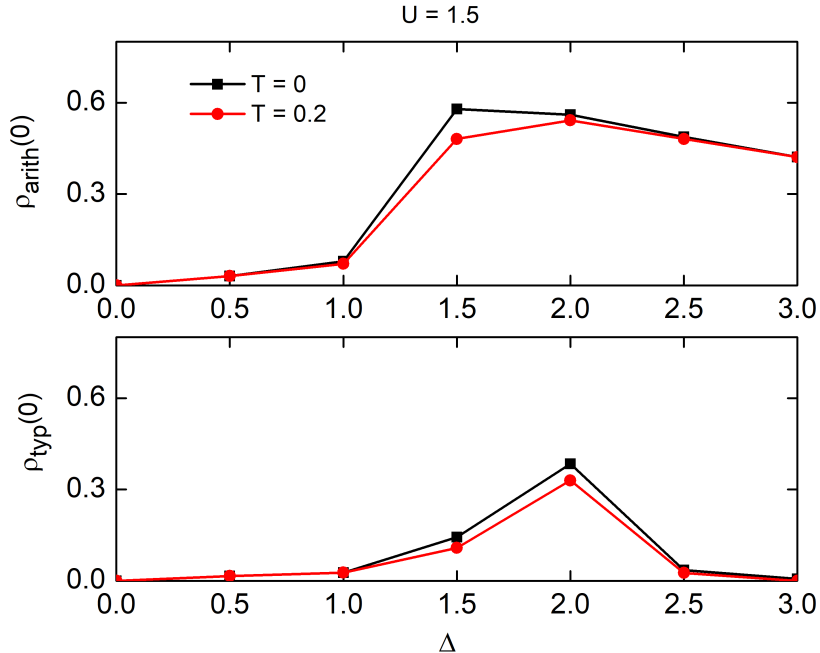


Figure 2. Arithmetic-averaged and typical DOS at the Fermi level as a function of disordered strength for $U = 1.5$ at $T = 0, 0.2$.

phase diagram consist of three phases: the correlated metal for small U and Δ , the Mott insulator for larger U , and the Anderson insulator for larger Δ . In addition, the boundaries between

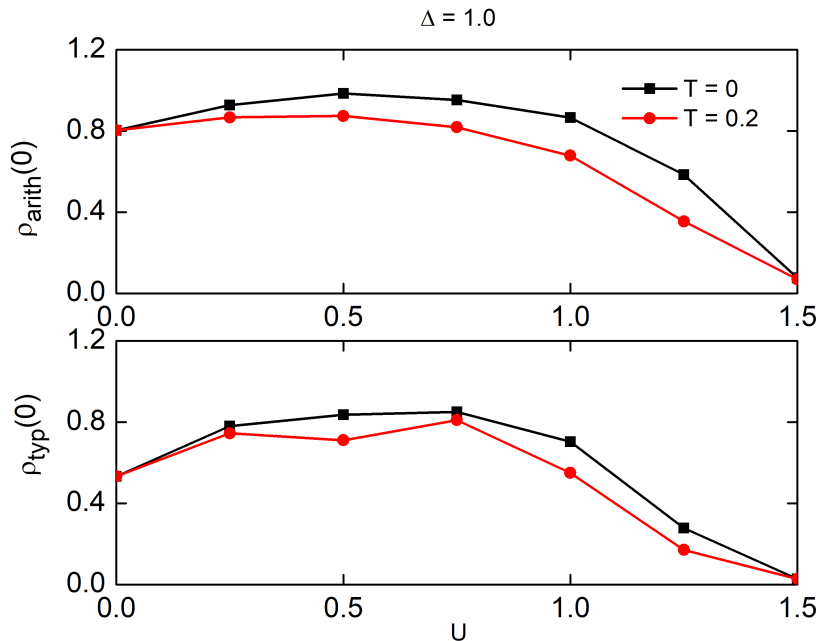


Figure 3. Arithmetic-averaged and typical DOS at the Fermi level as a function of disordered strength for $\Delta = 1.0$ at $T = 0, 0.2$.

these phases are almost unchanged compared to the case $T = 0$, because the critical interactions are very weakly dependent on temperature as noted above. We note that for the half-filling system the chemical potential is not affected by temperature due to particle-hole symmetry and that seems to be one reason why the phase diagram is almost temperature independent. In addition, although the temperature seemingly does not affect in the phase diagram, our obtained electronic properties of the system, for example, the dc conductivity is still clearly temperature dependent (not shown). The phase diagram of the half-filled AHM at finite temperature have been investigated in Ref. [14] within TMT-DMFT with the IPT impurity solver. The main effect of finite temperature is that the metal-insulator coexistence region is narrowed as temperature increases, and it vanishes at the critical temperature T_c . There is no coexistence region in our obtained phase diagrams using TMT-DMFT with the EOM impurity solver at zero and finite temperatures. However, as well as the case $T = 0$, we find that our obtained phase diagram at finite temperature is generally consistent with others at finite and zero temperatures [8, 10, 14]. Finally, in Fig.6 we plot an example of the site occupation as a function of the on-site energy, normalized by the disordered strength Δ for $U = 1.5$ at $T = 0.2$. For $\Delta = 0.5$ the system is in the Mott insulating phase, so the site occupation of all sites approximately equals 1.0; for the metallic ($\Delta = 1.5$) and the Anderson insulating phases ($\Delta = 3.5$), the site occupation changes from site to site, where in the latter case the change occurs more rapidly. Our result on the site occupation is in good agreement with those in Ref. [14].

4. Conclusions

In summary, we have studied the finite-temperature phase diagram of the half-filled AHM by using TMT-DMFT with EOM as an impurity solver. The results show that although

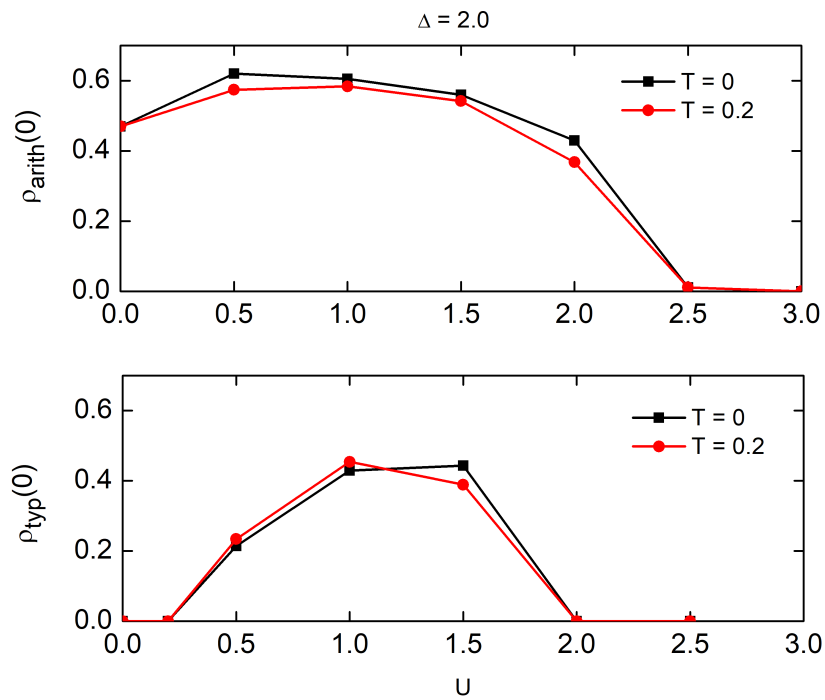


Figure 4. Arithmetic-averaged and typical DOS at the Fermi level as a function of disordered strength for $\Delta = 2.0$ at $T = 0, 0.2$.

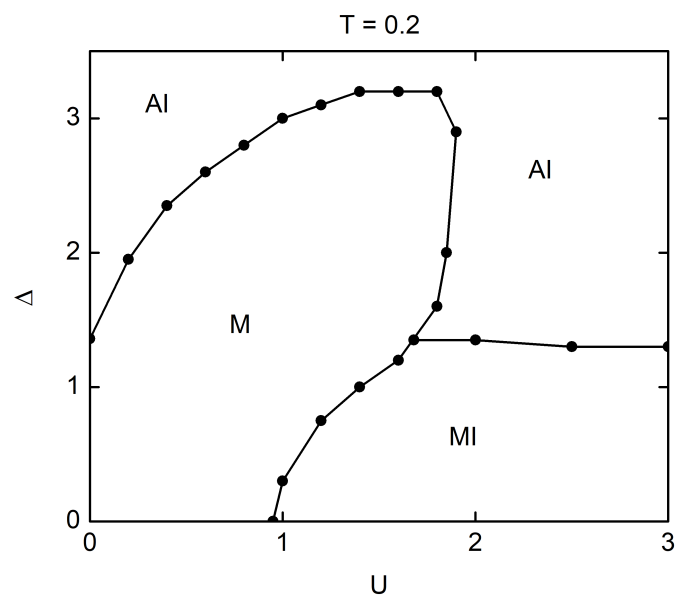


Figure 5. Phase diagram of the half-filled AHM at $T = 0.2$. M, MI and AI stand for metal, Mott insulator and Anderson insulator, respectively.

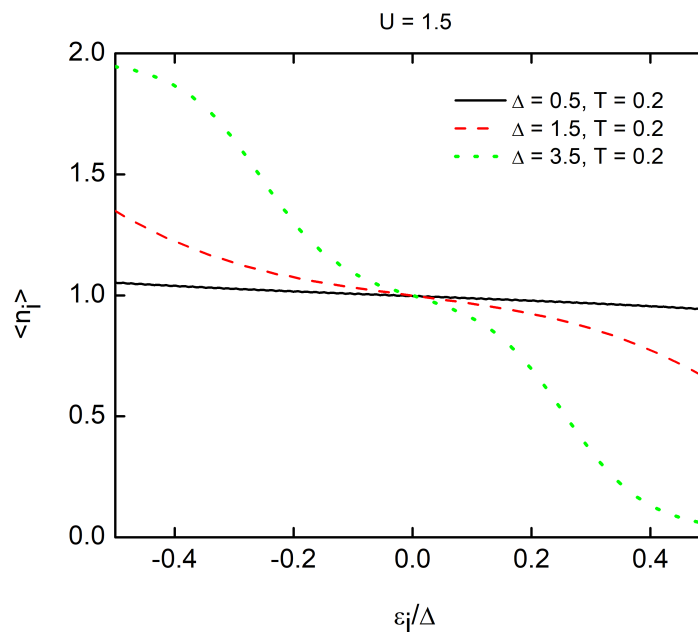


Figure 6. Site occupation as a function of the on-site energy, normalized by the disordered strength Δ for $U = 1.5$ at $T = 0.2$

the metallicity characterized by the value of the TDOS at the Fermi level in the correlated metallic region changes with temperature change, the boundaries between the metallic, Mott and Anderson insulating phases are almost temperature independent. We also have shown that for the system in the Mott insulating phase, the site occupation of all sites approximately equals 1.0, while for the metallic and the Anderson insulating phases, the site occupation changes from site to site, where in the latter case the change occurs more rapidly.

The Anderson-Hubbard model at finite temperature including the transport properties needs further investigation. That issue we will be working on in the near future.

Acknowledgments

This work is supported by International Centre of Physics ICP.2022.16

References

- [1] Mott N F 1949 *Proc. Phys. Soc. Lond. A* **62** 416.
- [2] Imada M, Fujimori A, and Tokura Y 1998 *Rev. Mod. Phys.* **70** 1039.
- [3] Anderson P W 1958 *Phys. Rev.* **109** 1492.
- [4] Lloyd P 1969 *J. Phys. C* **2** 1717.
- [5] Wegner F 1981 *Z. Phys. B* **44** 9.
- [6] Dobrosavljevic V, Pastor A A, and Nikolic B. K. 2003 *Europhys. Lett.* **62** 76.
- [7] Byczuk K 2005 *Phys. Rev. B* **71** 205105.
- [8] Aguiar M C O, Dobrosavljevic V, Abrahams E and Kotliar G 2009 *Phys. Rev. Lett.* **102** 156402
- [9] Byczuk K, Hofstetter W, and Vollhardt D 2010 *Inter. J. Mod. Phys. B* **24** 1727.
- [10] Byczuk K, Hofstetter W, and Vollhardt D 2005 *Phys. Rev. Lett.* **94** 0564021.
- [11] Hoang A T, Nguyen T H Y, and Le D A 2019 *Physica B* **570** 320.
- [12] Hoang A T, Nguyen T H Y, and Le D A 2021 *Mod. Phys. Lett. B* **35** 2150357.
- [13] Nguyen T H, Le D A, and Hoang A T 2022 *New J. Phys.* **24** 053054.
- [14] Braganca H, Aguiar M C O, Vucicevic J, Tanaskovic D, and Dobrosavljevic V 2015 *Phys. Rev. B* **92** 125143.
- [15] Meir y, Wingreen N S, and Lee P A 1991 *Phys. Rev. Lett.* **66** 3048.